Loss of E-Cadherin Promotes Metastasis via Multiple Downstream Transcriptional Pathways

Tamer T. Onder,[1,2] Piyush B. Gupta,[2,3] Sendurai A. Mani,[1] Jing Yang,[4] Eric S. Lander,[1,2,3,5] and Robert A. Weinberg[1,2]

[1]Whitehead Institute for Biomedical Research; [2]Department of Biology, Massachusetts Institute of Technology; and [3]Broad Institute of MIT and Harvard, Cambridge, Massachusetts; [4]Department of Pharmacology and Pediatrics, University of California, San Diego, School of Medicine, La Jolla, California; and [5]Department of Systems Biology, Harvard Medical School, Boston, Massachusetts

Abstract

Loss of the epithelial adhesion molecule E-cadherin is thought to enable metastasis by disrupting intercellular contacts—an early step in metastatic dissemination. To further investigate the molecular basis of this notion, we use two methods to inhibit E-cadherin function that distinguish between E-cadherin's cell-cell adhesion and intracellular signaling functions. Whereas the disruption of cell-cell contacts alone does not enable metastasis, the loss of E-cadherin protein does, through induction of an epithelial-to-mesenchymal transition, invasiveness, and anoikis resistance. We find the E-cadherin binding partner β-catenin to be necessary, but not sufficient, for induction of these phenotypes. In addition, gene expression analysis shows that E-cadherin loss results in the induction of multiple transcription factors, at least one of which, Twist, is necessary for E-cadherin loss–induced metastasis. These findings indicate that E-cadherin loss in tumors contributes to metastatic dissemination by inducing wide-ranging transcriptional and functional changes. [Cancer Res 2008;68(10):3645–54]

Introduction

On progression to high-grade neoplasia, cancer cells acquire qualities that enable them to invade neighboring tissues and, ultimately, to metastasize. The steps involved in metastatic dissemination include loss of cell-cell adhesion, increased motility and invasiveness, entry into and survival in the circulation, dispersion to distant anatomic sites, extravasation, and colonization of some of those sites (1). Whereas significant progress has been made in identifying molecular alterations responsible for primary tumor growth, the signaling pathways that regulate metastatic progression are less clear.

One protein prominently associated with tumor invasiveness, metastatic dissemination, and poor patient prognosis is the epithelial cell adhesion molecule E-cadherin (2–4). The significance of E-cadherin for metastasis has been shown in a variety of *in vitro* and *in vivo* models (5–8). E-Cadherin is a single-span transmembrane glycoprotein that establishes homophilic interactions with adjacent E-cadherin molecules expressed by neighboring cells, thereby forming the core of the epithelial adherens junction (9, 10).

In its cytoplasmic domain, E-cadherin associates with a number of proteins, including three catenins (α, β, and p120), which link E-cadherin to the actin cytoskeleton.

In light of its well-established function in maintaining adherens junctions, E-cadherin loss ostensibly promotes metastasis by enabling the first step of the metastatic cascade: the disaggregation of cancer cells from one another. However, it has been unclear whether E-cadherin loss also supports the successful completion of additional steps of the invasion-metastasis cascade. Previous work has revealed that several structural proteins associated with adherens junctions can also mediate intracellular signaling functions (11–14). Accordingly, E-cadherin loss may result in the activation of specific downstream signal transduction pathways that, in turn, confer traits on cancer cells facilitating completion of the later steps of metastasis.

In human tumors, loss or reduction of E-cadherin expression can be caused by somatic mutations, chromosomal deletions, proteolytic cleavage, and silencing of the *CDH1* promoter (15–18). Such silencing can occur either by DNA hypermethylation or through the action of transcription factors such as Slug, Snail, and Twist (19–22). These transcription factors were initially identified because of their role in mesoderm development, where they trigger epithelial-to-mesenchymal transitions (EMT) that involve, among other changes, the repression of E-cadherin expression (23). It has also become increasingly evident that these transcription factors play important roles in tumor progression (24). Given the known correlation between loss of E-cadherin expression and the up-regulation of these transcription factors, we were interested in learning whether the loss of E-cadherin is just one manifestation of the multicomponent EMT program that is activated in tumors or whether, alternatively, E-cadherin itself acts as a pleiotropic regulator of cell phenotype, enabling it to function as a master regulator of cell behavior.

In the present work, we examine whether loss of cell-cell contacts is the sole contribution to metastasis provided by E-cadherin loss. We find, instead, that multiple transcriptional pathways are activated on E-cadherin loss, at least two of which contribute to the later steps of metastatic dissemination. Thus, our findings reveal a complex transcriptional network that is controlled by the E-cadherin molecule.

Materials and Methods

Cell culture. Immortalized human breast epithelial cells (HMLE), generated through the introduction of the SV40 large T antigen, and hTERT were maintained as described (25). To generate tumorigenic and green fluorescent protein (GFP)–expressing derivates, we infected HMLE cells with pBabe H-ras and PRRL-GFP vectors (25). To measure cell growth rates, 2,500 cells were seeded onto 96-well plates in triplicate. Cell viability was measured using CellTiter-Glo (Promega) according to the

manufacturer's instructions. Treatment with the glycogen synthase kinase (GSK) inhibitor BIO (Calbiochem) was done for 6 h at 1 μmol/L concentration.

Plasmids. Sequences targeting the E-cadherin and β-catenin shRNAs were taken from the website of the RNAi consortium at the Broad institute and cloned into the PLKO-puro and PLKO-hygro vectors[6] (26). E-Cadherin and β-catenin targeting sequences are GCAGAAATTATTGGGCTCTTT and GCTTGGAATGAGACTGCTGAT, respectively. Control shRNAs were either targeted against GFP or a nonfunctional E-cadherin shRNA. Twist shRNA expression vector was previously described (22). Wild-type and dominant-negative mutant E-cadherin cDNAs (gifts of Dr. Gerhard Christofori, Department of Clinical Biological Sciences, University of Basel, Basel, Switzerland) were expressed from the pWZL-blasticidin vector. pBp-ΔN90β-catenin vector was used as described (27).

Viral production and infection of target cells. Viral production and infection of target cells were previously described (26). Infected cells were selected with 2 μg/mL puromycin, 200 μg/mL hygromycin, and 10 μg/mL blasticidin.

Antibodies, immunoblotting, immunofluorescence, and histology. Antibodies used were E-cadherin, α-catenin, β-catenin, γ-catenin, N-cadherin (BD Transduction), phospho-β-catenin, phospho-GSK3β, GSK3β (Cell Signaling), vimentin V9 (NeoMarkers), actin, tubulin (Abcam), H-Ras (Santa Cruz Biotechnology), fibronectin (Sigma), and cytokeratin 8 (Troma-1, Developmental Studies Hybridoma Bank, University of Iowa). Twist monoclonal antibody was used as previously described (22). For immunohistochemical staining, anti–large T antigen (Santa Cruz Biotechnology) and anti–E-cadherin (Cell Signaling) antibodies were used as described (25).

Anoikis assays. Cells (75,000) were seeded onto six-well ultra-low attachment plates. After 24 or 48 h, cells were harvested and incubated at 37°C with 0.25% trypsin for 5 min to prevent cell aggregation. Viable cells were counted using trypan blue. For fluorescence-activated cell sorting (FACS) analysis, we used the ApoAlert Annexin V-FITC Apoptosis Kit (Takara-Bio) according to the manufacturer's instructions and used a FACSCalibur flow cytometer (Becton Dickinson).

Motility and invasion assays. Cells (5×10^5) were resuspended in a 1:1 mixture of DME:F12 and placed into uncoated or Matrigel-coated Transwell inserts containing 8-μm filters (BD Falcon) in triplicate. The bottom wells contained DME:F12 media with growth factors, insulin (10 μg/mL), epidermal growth factor (10 ng/mL), and hydrocortisone (1 μg/mL). After 12 or 16 h, the cells on the upper surface of the filters were removed with a cotton swab. The filters were fixed and stained with a Diff-Quick staining kit (Dade Behring) and photographed. The migrated cells were then counted.

***In vivo* tumorigenesis and metastasis assays.** Nonobese diabetic, severe combined immunodeficient (NOD-SCID) mice (propagated on site) and nude mice (NCR nude; Taconic) were used in these studies, and all protocols were approved by the Massachusetts Institute of Technology Committee on Animal Care. Nude mice received 400 rad of γ-radiation using a dual ^{137}Cs source 1 day before tumor cell injection. Mice were anesthetized with either avertin or isoflurane. For orthotopic injections, 1 million cells in 20 μL of Matrigel (Becton Dickinson), diluted 1:2 in DME, were injected into each of two mammary glands per female NOD-SCID mouse. For s.c. injections, 1×10^6 cells in 100 μL of Matrigel diluted 1:2 in DME were injected at each of two sites per nude mouse. Tumor diameters were measured biweekly using precision calipers. Primary tumor–bearing animals were sacrificed when the tumors reached a diameter of 2 cm. For tail vein injections, 5×10^5 cells in 200-μL PBS were injected per NOD-SCID mouse and the mice were sacrificed 8 wk postinjections.

Visualization and quantification of GFP-labeled lung metastases. On necropsy, lungs of injected mice were removed and examined under a Leica MZ 12 fluorescence dissection microscope. Images of lung lobes were captured at identical settings. The amount of metastatic burden was quantified using ImageJ[7] and expressed as a percentage of the total lung area captured (28).

Microarray hybridization, data collection, and analysis. Total RNA was extracted from three independent culture plates for each cell type with an RNeasy Mini kit (Qiagen). Synthesis of cRNA and hybridization/scanning of microarrays were done with Affymetrix GeneChip products as described in the GeneChip manual. Normalization of the raw gene expression data, quality control checks, and subsequent analyses were done using the open-source R-project statistical software[8] (29) in conjunction with Bioconductor packages. Raw data files (.CEL) were converted into probe set values by RMA normalization. Hierarchical clustering with complete linkage was done on the probe set data using the Euclidean metric. The probes used for hierarchical clustering and heatmap generation were identified on the basis of their consistent up-regulation and down-regulation across a set of isogenic lines that were induced into EMT using a variety of inducers: Twist, TGF-β, Snail, or Goosecoid overexpression (to be described in detail elsewhere).[9] The identified probes constitute an EMT expression signature whose targets are >3-fold up-regulated or down-regulated in each of the cell lines induced into EMT relative to vector control cells that were not induced into EMT.[9] The microarray data have been deposited in National Center for Biotechnology Information Gene Expression Omnibus (GEO) and are accessible through GEO Series accession number GSE9691.

SYBR green real-time reverse transcription-PCR. Reverse transcription-PCR (RT-PCR) analysis of *twist* was carried out as described (22).

Results

Characterization of *in vitro* phenotypes resulting from expression of E-cadherin shRNA and dominant-negative E-cadherin. To resolve the role of E-cadherin in cell-cell adhesion from its intracellular signaling functions, we used two distinct methods of inhibiting E-cadherin function: (*a*) shRNA-mediated knockdown of E-cadherin, which resulted in >90% reduction of E-cadherin protein levels (shEcad), and (*b*) expression of a truncated form of E-cadherin (DN-Ecad) lacking the ectodomain of the wild-type protein (Fig. 1*A* and *B*). This truncation product, which retains the cytoplasmic domain, has previously been shown to act in a dominant-negative manner by binding and titrating cytoplasmic proteins associated with the adherens junctions, thereby abstracting them from wild-type E-cadherin molecules (30).

We expressed both constructs either in immortalized but untransformed human mammary epithelial cells (HMLE) or in *ras*-transformed derivatives (HMLER). Both types of cells expressing control shRNA (shCntrl) grew in monolayer culture as epithelial clusters with a typical cobblestone morphology, whereas knockdown of E-cadherin and expression of the dominant-negative protein both resulted in loss of cell-cell contacts and cell scattering (Fig. 1*A*). This was observed with both the HMLE and HMLER cells (Supplementary Fig. S1*A*).

Whereas the cell populations expressing shEcad and DN-Ecad both lost cell-cell adhesion, the individual cells expressing shEcad displayed, in addition, an elongated, fibroblastic morphology (Fig. 1*A*). To confirm that this phenotype was a specific consequence of E-cadherin ablation, we reexpressed E-cadherin in HMLE-shEcad cells. Indeed, expression of an shRNA-resistant murine E-cadherin gene reversed the observed phenotypes, causing shEcad cells to revert to an epithelial morphology and to regenerate a cobblestone growth pattern in monolayer culture (Supplementary Fig. S2).

---

[6] http://www.broad.mit.edu/genome_bio/trc/
[7] http://rsb.info.nih.gov/ij/

[8] http://www.r-project.org/
[9] Manuscript in preparation.

Figure 1. Characterization of *in vitro* phenotypes resulting from expression of E-cadherin shRNA and dominant-negative E-cadherin. *A,* schematic representation of the generation of HMLER-shCntrl, shEcad, and DN-Ecad cell lines, as well as their respective morphologies. *B.* expression levels of the endogenous and dominant-negative mutant E-cadherin (*arrowhead*), β-catenin, γ-catenin, α-catenin, cytokeratin-8 (*CK-8*), and mesenchymal proteins N-cadherin and vimentin in HMLER-shCntrl, shEcad, and DN-Ecad cells examined by immunoblotting. β-Actin is used as a loading control. *C,* immunofluorescence staining of E-cadherin (*green*), vimentin (*red*), and N-cadherin (*green*) in the HMLER cells expressing either shCntrl or shEcad. The blue signal represents the nuclear DNA staining by 4′,6-diamidino-2-phenylindole.
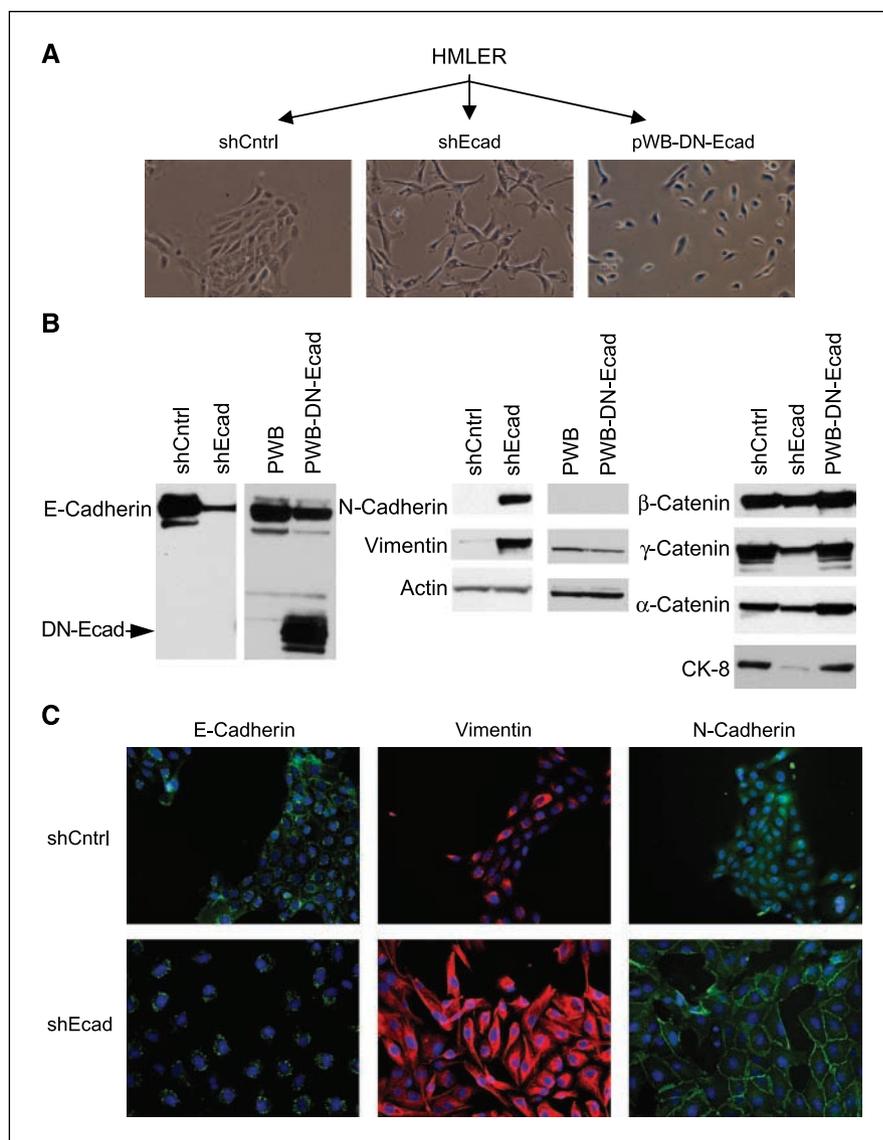
The acquisition of a fibroblastic morphology by the cells expressing shEcad suggested that these cells had undergone an EMT. To determine whether, in addition to the observed morphologic changes, the molecular alterations associated with an EMT occurred on loss of E-cadherin, we assessed the status of EMT markers in control, shEcad, and DN-Ecad HMLER cells. On shRNA-mediated loss of E-cadherin, expression of mesenchymal proteins such as N-cadherin and vimentin was markedly up-regulated (Fig. 1*B* and *C*). In contrast, none of the mesenchymal proteins was up-regulated in HMLER-DN-Ecad cells (Fig. 1*B*). Whereas the expression of adherens junction-associated catenins was maintained in the absence of E-cadherin, epithelial cytoker-atins were down-regulated (Fig. 1*B*). These observations indicate that complete loss of E-cadherin protein results in an EMT, whereas inhibition of E-cadherin–mediated cell-cell adhesion causes cell scattering without the additional changes in differen-tiation state associated with passage through the EMT program.

Primary tumor formation and metastatic competence of E-cadherin–inhibited cancer cells. To determine whether E-cadherin perturbation affects primary tumor growth, we injected control HMLER cells and the two E-cadherin–inhibited derivative lines s.c. into nude mice. Whereas all three cell lines generated primary tumors with comparable latencies, tumor growth rates differed slightly among shCntrl, DN-Ecad, and shEcad HMLER cells, with the latter growing most rapidly (Fig. 2*A*). We confirmed that E-cadherin suppression and expression of the dominant-negative construct were maintained during the course of tumor growth (Supplementary Fig. S3). Immunohistochemical staining of tumors with anti–E-cadherin antibodies also supported this conclusion (Supplementary Fig. S3).

We next determined whether metastatic dissemination to the lungs occurred when these various transformed cells were implanted in an orthotopic tissue site—the mammary fat pad. To facilitate detection of microscopic and macroscopic metastases, we engineered the introduced HMLER cells to express the GFP. We controlled for differences in primary tumor growth rates by sacrificing animals when their tumor burden reached a preestab-lished threshold. Accordingly, the mean primary tumor weights at the end of the experiment were comparable across the shCntrl, shEcad, and DN-Ecad cohorts (Fig. 2*B*).
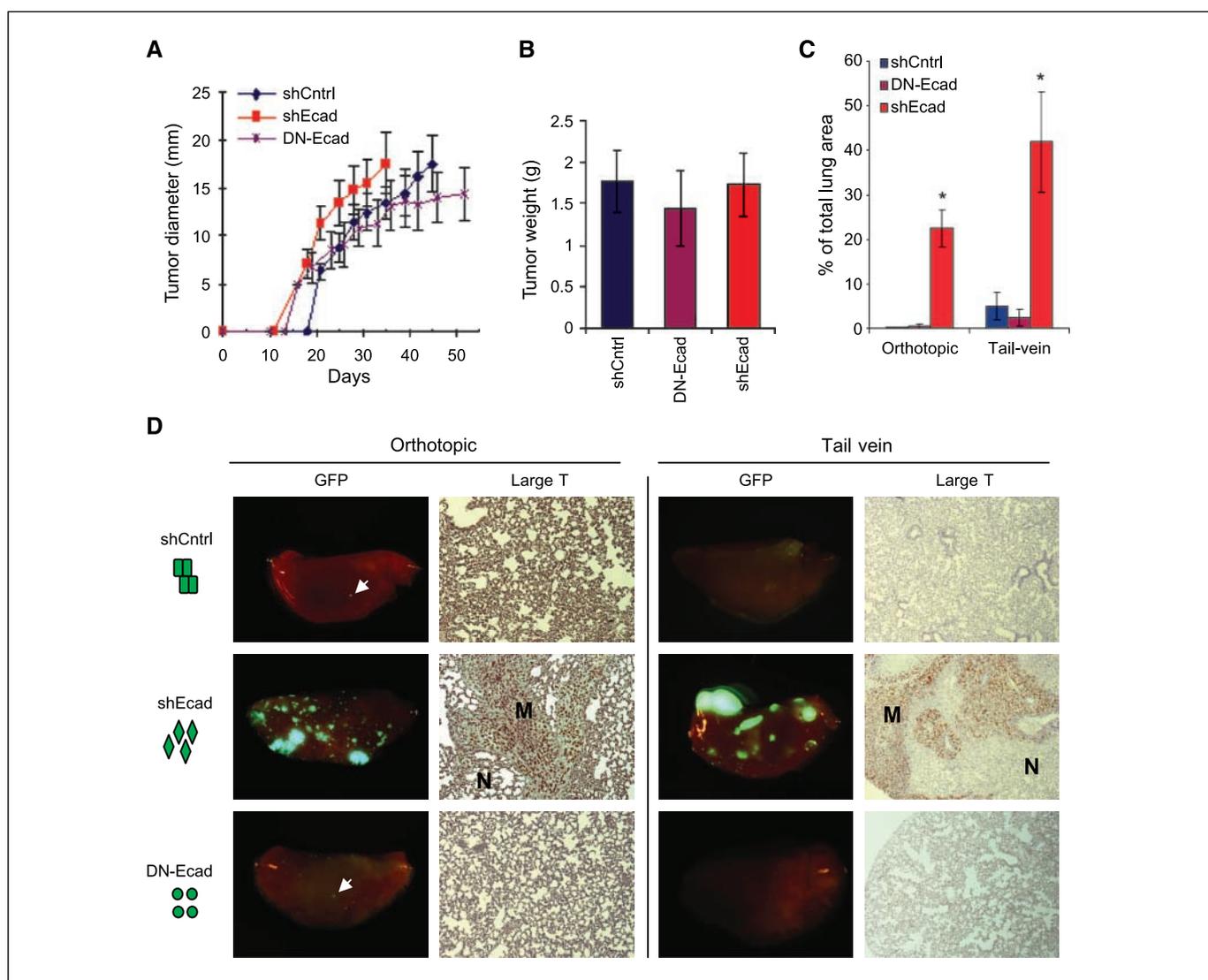
Figure 2. Loss of E-cadherin is sufficient for metastasis whereas cellular disaggregation is not. *A,* growth patterns of primary s.c. tumors formed by the HMLER-shCntrl, shEcad, and DN-Ecad cells. *Points,* mean of eight primary tumors; *bars,* SD. *B,* final primary tumor weights of HMLER-shCntrl, shEcad, and DN-Ecad tumors grown s.c. *Columns,* mean of eight primary tumors; *bars,* SD. *C,* quantification of total lung metastasis burden in mice bearing either orthotopic primary tumors of HMLER-shCntrl, shEcad, and DN-Ecad cells or 8 wk after tail-vein injection of these lines. *Columns,* mean of five mice analyzed per group; *bars,* SD. *, $P < 0.001$. *D,* representative fluorescence images of mouse lung lobes bearing either orthotopic primary tumors of HMLER-shCntrl, shEcad, and DN-Ecad cells or 8 wk after tail-vein injection of these lines. GFP signal denotes the presence of tumor cells (*left*). *Arrows,* occasional tumor cells detected in the lungs of control and DN-Ecad tumor–bearing animals. Representative immunohistochemical staining of sections with anti–large T antibody from the same set of lungs. Brown nuclear staining denotes the tumor cells. *N,* lung tissue; *M,* metastatic nodule (*right*).

In consonance with previous findings (25), control HMLER cells did not form any macroscopic nodules in the lungs, and only a few GFP-positive cells could be detected as micrometastases in the lungs of animals bearing these tumors (Fig. 2D). In contrast, animals bearing HMLER-shEcad tumors harbored numerous microscopic and macroscopic metastases in their lungs (Fig. 2D). In fact, the lung metastatic burden in animals bearing HMLER-shEcad tumors covered a substantial portion of the total lung surface (Fig. 2C and D). Whereas we did find small numbers of cells in the lungs of mice bearing HMLER-DN-Ecad tumors, macroscopic nodules were never observed. These results indicate that the two modes of E-cadherin inhibition yield cancer cells with qualitatively different metastatic powers.

Because the HMLER-DN-Ecad cells were incapable of forming macroscopic metastases from primary tumors growing at ortho-topic sites, we also subjected these cells to a less stringent test of metastatic competence—the "experimental metastasis" model, which involves tail vein injection of tumor cells. Using this assay, HMLER-shCntrl cells rarely formed macroscopic nodules in the lungs after an 8-week incubation period (2 nodules in 1 of 5 mice; Fig. 2C and D). In contrast, HMLER-shEcad cells established numerous lung macrometastases, some of which invaded the rib cage. However, DN-Ecad cells did not form either microscopic or macroscopic lung nodules in any of the mice, thereby echoing the previous results (Fig. 2D).

Taken together, these observations suggest that whereas the loss of cell-cell contacts does not suffice to impart metastatic competence to cancer cells, the concomitant liberation of adherens junction proteins and other associated proteins from the cytoplasmic tail of E-cadherin indeed suffices to do so. Hence, in

addition to promoting dissemination from primary tumor sites via the disruption of cell-cell contacts, E-cadherin loss facilitates the successful completion of one or more subsequent rate-limiting steps of the invasion-metastasis cascade.

Functional differences in cell motility, invasion, and anoikis resistance. To determine the functional changes in cell behavior that occurred following E-cadherin loss, we used several *in vitro* assays to characterize the control and E-cadherin–perturbed HMLER cells. More specifically, we used Boyden chamber assays to gauge the migratory and invasive abilities of these various cells. Whereas control cells were minimally motile and invasive, E-cadherin loss resulted in a significant increase in both motility and invasiveness (Fig. 3*A* and *B*). However, DN-Ecad cells, whereas more motile than controls (albeit less so than shEcad cells), failed to invade through Matrigel-coated membranes.

Disseminating tumor cells that enter into the bloodstream lose their attachment to the extracellular matrix, resulting in induction of the form of apoptosis termed anoikis (1). Moreover, expression of antiapoptotic molecules that confer resistance to anoikis has been shown to promote metastasis (31, 32). We therefore set out to evaluate the anoikis sensitivity of DN-Ecad, shEcad, and control HMLER cells. When placed into suspension cultures, the viability of both control and DN-Ecad cells declined dramatically over a 2-day period (Fig. 3*C*); in contrast, shEcad cultures exhibited only a minor

decrease in cell number during the same time period (Fig. 3*C*). To confirm that loss of viability was indeed a consequence of increased apoptosis, we stained cells from these cultures with Annexin V. Whereas the control and DN-Ecad suspension cultures exhibited a significant fraction of cells undergoing apoptosis, minimal Annexin V positivity was observed in the shEcad cultures (Fig. 3*D*).

Taken together, these results indicate that EMT induction upon E-cadherin loss promotes cancer cell invasiveness and enables survival in the absence of substrate attachment. Importantly, the acquisition of these traits was not a direct consequence of the disruption of cell-cell adhesion per se, suggesting that activation of specific signaling pathways following E-cadherin loss is important for the observed phenotypes.

The role of β-catenin in EMT and metastasis induced by E-cadherin loss. A critical intracellular protein associated with the E-cadherin cytoplasmic tail is β-catenin, which has previously been implicated in the induction of EMTs in various contexts (33–38). We therefore examined whether E-cadherin loss influenced β-catenin status and whether such change in β-catenin contributed, in turn, to the subsequent induction of EMT. Whereas in control cells β-catenin localization was predominantly associated with cell-cell junctions, shEcad cells exhibited a diffuse cytoplasmic and nuclear localization pattern (Fig. 4*A*). Examination of the phosphorylation status of β-catenin in shEcad cells indicated that
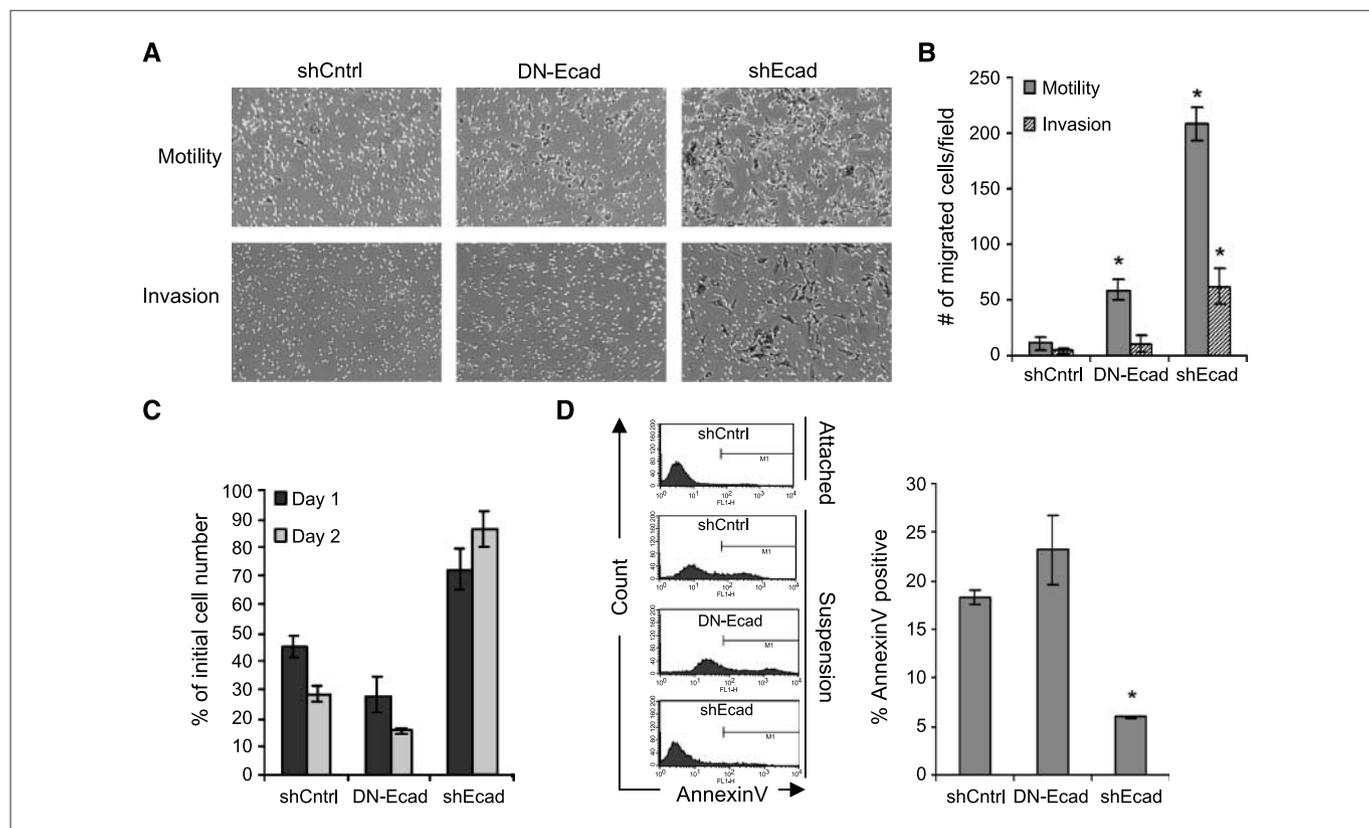

Figure 3. Loss of E-cadherin leads to increased invasiveness and resistance to anoikis. *A,* HMLER-shCntrl, shEcad, and DN-Ecad cells were induced to move or invade through uncoated or Matrigel-coated transwell membranes. After 12 h (uncoated) or 16 h (Matrigel-coated), the migrated cells were fixed, stained, and photographed. Representative photographs of Transwell membranes showing stained migrated cells from either motility or invasion experiments. *B,* quantification of motility and invasion experiments (*A*) done by counting the number of migrated cells. *Columns,* mean of triplicate assays; *bars,* SD. *, *P* < 0.01, compared with shCntrl. *C,* HMLER-shCntrl, shEcad, and DN-Ecad cells were put in suspension and cultured on ultra-low attachment plates in triplicate. After the indicated times, viable cells were counted with trypan blue. *Columns,* mean number of remaining viable cells expressed as a percentage of the initial seeding; *bars,* SD. *D,* representative FACS histograms indicating the percentage of apoptotic HMLER-shCntrl, shEcad, and DN-Ecad cells in suspension as determined by binding of FITC-conjugated Annexin V. The FACS analyses were done 24 h after suspension culture. *Right, columns,* mean number of Annexin V–positive cells expressed as a percentage of total cells; *bars,* SD. *, *P* < 0.001.

it was largely unphosphorylated, and therefore present in an active state (Fig. 4*A*; ref. 13). In contrast, a significant amount of β-catenin protein in control cells was phosphorylated and thus targeted for ubiquitylation and degradation (Fig. 4*A*).

We next determined whether the observed β-catenin phosphorylation was correlated with the state of GSK-3β, the kinase that is primarily responsible for phosphorylating it, thereby labeling it for subsequent ubiquitylation. Indeed, we found that GSK-3β was largely in a phosphorylated, and therefore inactive, state in HMLER-shEcad cells, in contrast to its unphosphorylated state in control cells (Fig. 4*A*; ref. 39). Hence, loss of E-cadherin in HMLER cells was sufficient to liberate β-catenin from its site of sequestration adjacent to the plasma membrane and to permit its survival in an unphosphorylated, stabilized state.

To determine whether β-catenin was functionally active following E-cadherin loss, we inhibited β-catenin expression in HMLER-shEcad cells using a lentiviral shRNA vector (shEcad + shBcat; Fig. 4*B*). Down-regulation of β-catenin resulted in a slightly reduced growth rate *in vitro* (Supplementary Fig. S4). Importantly, β-catenin knockdown in shEcad cells significantly diminished expression of the mesenchymal proteins N-cadherin, vimentin, and fibronectin (Fig. 4*B*). In contrast, the down-regulation of epithelial cytokeratins in shEcad cells still occurred in the absence of β-catenin (Fig. 4*B*).

We next assessed whether β-catenin affected cell biological phenotypes associated with metastasis. β-Catenin inhibition in shEcad cells decreased cancer cell invasiveness (Fig. 4*C*). In addition, knockdown of β-catenin sensitized shEcad cells to apoptosis specifically when the cells were placed in a suspension culture
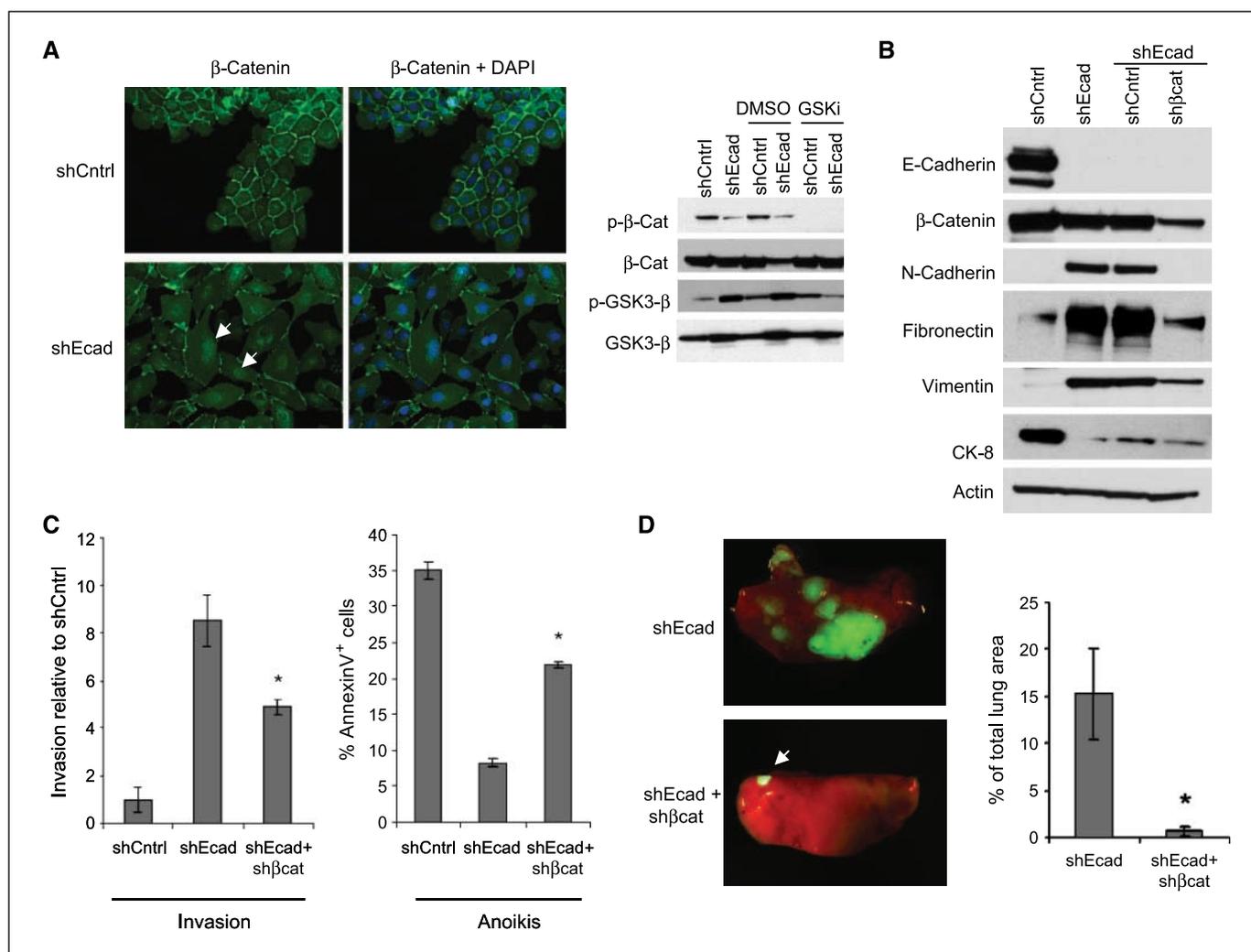

Figure 4. β-Catenin is activated on E-cadherin loss and is necessary for E-cadherin–induced EMT. *A,* immunofluorescence staining for β-catenin (*green*) in shCntrl and shEcad cells showing differential localization. *Right,* nuclear 4′,6-diamidino-2-phenylindole (*DAPI*; *blue*) staining of the same cells. *White arrows,* nuclear β-catenin staining observed in the shEcad cells. Immunoblots showing phospho-β-catenin, total β-catenin, phospho-GSK3β, and total GSK levels in either untreated shCntrl and shEcad cells or in the same set of cells treated with DMSO or GSK inhibitor BIO (1 μmol/L) for 6 h. *B,* expression levels of E-cadherin, β-catenin, E-cadherin, N-cadherin, and vimentin in HMLER-shCntrl, shEcad, and double knockdown cells (shEcad + shβcat) cells examined by immunoblotting. β-Actin is used as a loading control. *C, left,* HMLER-shCntrl, shEcad, and shEcad + shβcat cells were induced to invade through Matrigel-coated transwell membranes. After 16 h, the invaded cells were fixed, stained, photographed, and counted. *Columns,* mean of triplicate assays, shown relative to shCntrl cell invasion; *bars,* SD. *, $P < 0.01$, compared with shEcad. *Right,* the percentage of apoptotic HMLER-shCntrl, shEcad, and shEcad + shβcat cells in suspension was determined by binding of FITC-conjugated Annexin V. The FACS analyses were done 24 h after suspension culture. *Columns,* mean number of Annexin V–positive cells expressed as a percentage of total cells; *bars,* SD. *, $P < 0.01$, compared with shEcad. *D,* representative fluorescence images of mouse lung lobes 8 wk after tail-vein injection of shEcad or shEcad + shβcat cells. GFP signal denotes the presence of tumor cells (*left*). Quantification of total lung metastasis burden in the same sets of mice. *Right, columns,* mean of seven mice analyzed; *bars,* SD. *, $P < 0.001$.
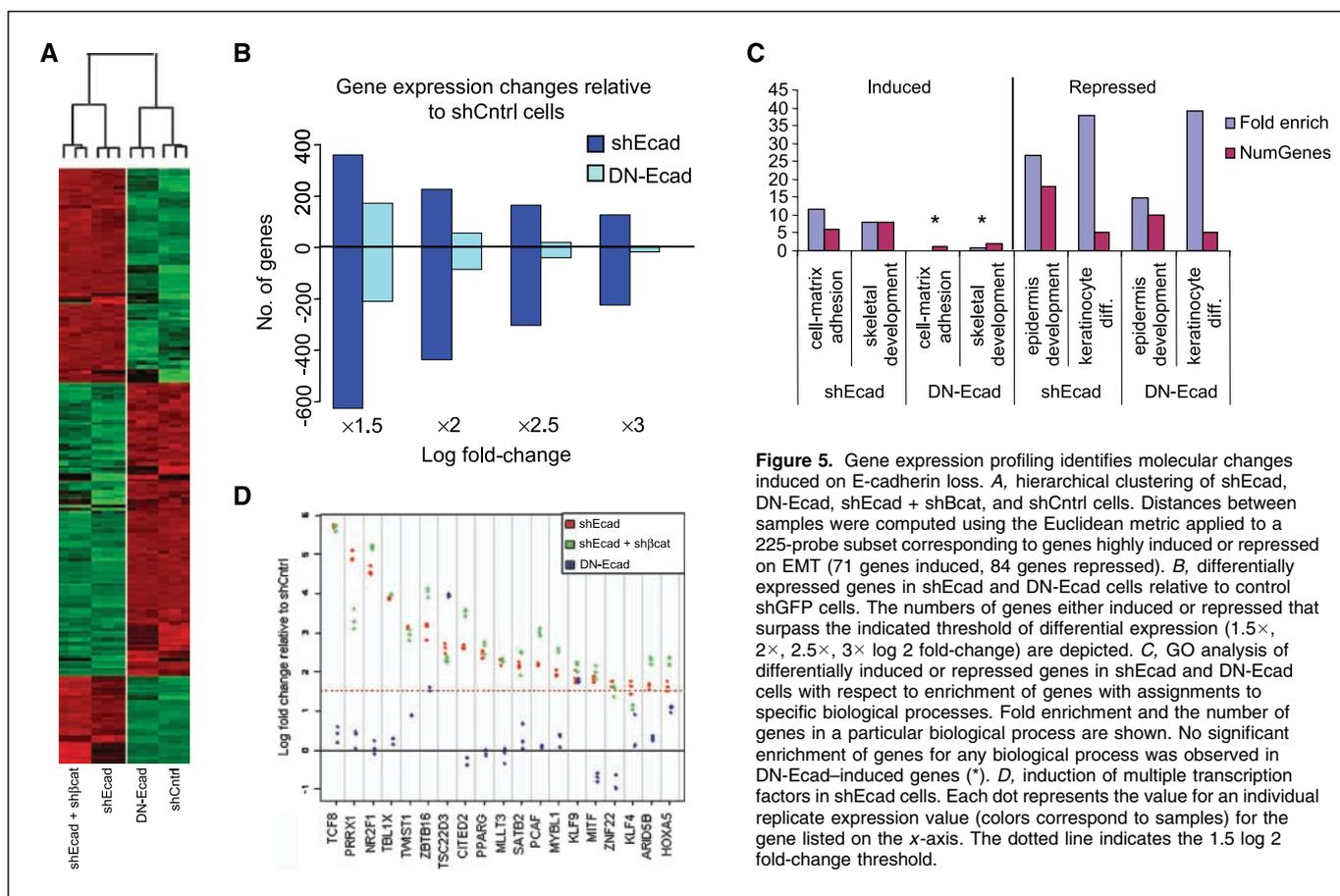
Figure 5. Gene expression profiling identifies molecular changes induced on E-cadherin loss. *A,* hierarchical clustering of shEcad, DN-Ecad, shEcad + shBcat, and shCntrl cells. Distances between samples were computed using the Euclidean metric applied to a 225-probe subset corresponding to genes highly induced or repressed on EMT (71 genes induced, 84 genes repressed). *B,* differentially expressed genes in shEcad and DN-Ecad cells relative to control shGFP cells. The numbers of genes either induced or repressed that surpass the indicated threshold of differential expression (1.5×, 2×, 2.5×, 3× log 2 fold-change) are depicted. *C,* GO analysis of differentially induced or repressed genes in shEcad and DN-Ecad cells with respect to enrichment of genes with assignments to specific biological processes. Fold enrichment and the number of genes in a particular biological process are shown. No significant enrichment of genes for any biological process was observed in DN-Ecad–induced genes (*). *D,* induction of multiple transcription factors in shEcad cells. Each dot represents the value for an individual replicate expression value (colors correspond to samples) for the gene listed on the x-axis. The dotted line indicates the 1.5 log 2 fold-change threshold.

(Fig. 4*C*). To assess the contribution, if any, of β-catenin to the metastatic behavior of shEcad cells, we introduced control shEcad and double knockdown (shEcad + shβcat) cells via the tail vein directly into the circulation. We observed that HMLER + shEcad + shβcat cells were significantly impaired in their ability to form lung metastases compared with HMLER + shEcad cells (Fig. 4*D*).

Because β-catenin was necessary for various aspects of the EMT occurring following E-cadherin loss, we examined whether β-catenin activation would, on its own, suffice to induce EMT. Overexpression of a constitutively active β-catenin protein did not induce the expression of any mesenchymal markers examined (Supplementary Fig. S5). Taken together, these data indicate that whereas β-catenin was required for changes in the expression of certain biochemical markers associated with the EMT as well as for acquisition of traits facilitating metastasis, it does not suffice on its own to induce these phenotypes.

Gene expression profiling identifies global changes resulting from E-cadherin loss. To obtain an unbiased view of the molecular changes resulting from the liberation of intracellular adherens junction proteins from the cytoplasmic domain of E-cadherin, we compared the gene expression profiles of shEcad, DN-Ecad, and control cells. To avoid the influence of specific oncogenic lesions, we used the immortalized, nontransformed mammary epithelial (HMLE) cells for this analysis. Furthermore, we reasoned that a comparison between shEcad- and DN-Ecad–expressing cells would make it possible to identify those changes in gene expression that were not consequences of the loss of cell-cell adhesion. In addition, we incorporated into this analysis the expression profile of cells in

which both E-cadherin and β-catenin were inhibited; this would allow us to evaluate the contribution of β-catenin to the gene expression changes observed following inhibition of E-cadherin.

The global expression profiles revealed that shEcad cells exhibited significantly greater overall differential gene expression relative to control cells than did DN-Ecad cells (Fig. 5*A* and *B*; see Supplementary Tables S1 and S2 for complete lists). Nonetheless, there was an overlap between the genes that were differentially expressed in both shEcad and DN-Ecad cells relative to control cells (18 induced and 59 repressed; Supplementary Table S3). This indicated that the loss of cell-cell contacts, on its own, suffices to alter expression of this subset of cellular genes.

Among the genes significantly induced in shEcad cells relative to controls were a number of mesenchymal markers known to be associated with passage through an EMT, including N-cadherin, vimentin, fibronectin, and seven distinct collagens. In addition to these induced mesenchymal markers, 11 distinct cytokeratin genes were down-regulated in shEcad cells (Supplementary Table S1) relative to controls. Whereas none of the above-mentioned mesenchymal genes was induced in cells expressing DN-Ecad, we did observe down-regulation of 4 of the 11 cytokeratin genes in DN-Ecad–expressing cells.

We further analyzed these changes by testing for their association with the biological processes arrayed in the Gene Ontology (GO) database (40). Genes most significantly down-regulated in shEcad and DN-Ecad cells were, in both cases, strongly associated with cell differentiation (Fig. 5*C*). Whereas the genes induced in shEcad cells were strongly associated with matrix

adhesion and skeletal development, the genes induced in DN-Ecad cells were not significantly associated with any specific biological processes listed in the GO database (Fig. 5C). This indicated that down-regulation of certain epithelial genes results directly from the dissolution of cell-cell contacts, and that the induction of mesenchymal characteristics required, in addition, the loss of the cytoplasmic domain of E-cadherin.

To directly assess the extent to which of these various cell lines had entered into a mesenchymal state, we performed hierarchical clustering on the expression data using a global metric computed on the basis of a 225-gene set capable of discriminating between mammary epithelial cells that have or have not been induced to undergo EMT by a variety of means, including the expression of the Snail and Twist transcription factors.[10] This analysis revealed that the expression profiles of the control and DN-Ecad cell lines were essentially indistinguishable with respect to these EMT-associated genes and were both indicative of cells that have not undergone an EMT (Fig. 5A). In contrast, the expression profile of shEcad cells indicated that they had, in fact, passed through an EMT (Fig. 5A). These findings reinforced our earlier conclusion that shEcad cells, but not DN-Ecad cells, have indeed adopted a mesenchymal cell state.

Expression of multiple transcription factors is induced on E-cadherin loss but not cell-cell disaggregation. To evaluate the contribution of β-catenin to the gene expression changes observed on E-cadherin loss, we compared the expression profile of the doubly altered cells (HMLE shEcad + shβcat) with the profile of shEcad cells. We observed that ∼14% of the genes (84 of 617 genes; Supplementary Table S4) that were differentially expressed in shEcad cells relative to control cells were dependent on β-catenin for their regulation. The β-catenin dependence of a number of representative genes induced or repressed by E-cadherin loss is depicted in Supplementary Fig. S6.

Because 84% of the gene expression changes that occurred on E-cadherin loss were not dependent on β-catenin function, it was likely that other transcriptional regulators were mediating the transcriptional changes following E-cadherin loss. In fact, there were 19 transcription factors that were up-regulated >3-fold in shEcad cells relative to control cells (Fig. 5D). Of these factors, only two were up-regulated in DN-Ecad cells, indicating that induction of the remaining 17 required the loss of the cytoplasmic tail of E-cadherin. In light of the observation that β-catenin is incapable on its own of inducing EMT, these findings further implicated one or more of these 19 factors as potential contributors to the EMT observed following E-cadherin loss.

Up-regulation of Twist on loss of E-cadherin and its functional role. The presence of the transcription factors *twist* and *TCF8 (ZEB-1)* among the set of genes highly up-regulated on E-cadherin loss was surprising (Fig. 5D). Twist had previously been shown to be essential for the metastasis of mouse mammary tumor cells and to be expressed in a high proportion of human lobular breast cancers in correlation with E-cadherin down-regulation (22). Twist is functionally related to a set of transcription factors, including Snail, Slug, SIP1, and ZEB-1, which are known to repress E-cadherin expression and are sufficient in various cellular contexts to induce EMTs. Based on extensive previous work, these factors are thought to act upstream of E-cadherin, and several are

known to directly repress transcription of the *CDH1* gene itself (20, 41–44).

The identification of Twist and ZEB-1 in our gene expression data suggested the opposite possibility—that the expression of EMT-inducing transcription factors may, under certain circumstances, be controlled by the levels of E-cadherin. We pursued this hypothesis by examining the functional consequences of Twist induction following E-cadherin loss. Analyses of *twist* mRNA levels by real-time RT-PCR validated the expression array data, indicating that *twist* was specifically up-regulated in HMLER-shEcad but not in control or DN-Ecad cells (Fig. 6A).

To determine whether Twist expression played a functionally important role in the EMT induced upon E-cadherin loss, we superinfected shEcad cells with a lentiviral shRNA vector targeting Twist. Introduction of this shRNA vector resulted in an ∼5-fold decrease in Twist levels, reducing it below the basal levels present in the parental HMLER line (Fig. 6B). Whereas Twist inhibition led to a ∼50% reduction of N-cadherin levels, the expression of vimentin remained largely unaffected (Fig. 6B).

To further evaluate the functional consequences of Twist up-regulation to metastasis-associated traits, we characterized the contribution of Twist to the induction of invasion and anoikis resistance following E-cadherin loss. Twist inhibition resulted in a significant reduction in the invasive behavior of shEcad cells (Fig. 6C). In addition, sensitivity to induction of anoikis was partially restored upon Twist inhibition (Fig. 6C). These findings indicated that Twist is an important mediator of signaling in response to E-cadherin loss and operates upstream of certain cellular functions that contribute to metastatic competence. The observed effects on motility, invasiveness, and anoikis resistance following Twist knockdown were similar to those observed on β-catenin knockdown. Because the induction of Twist was not β-catenin dependent, we concluded that these two factors may be acting in parallel to program the cellular changes observed following E-cadherin loss.

To determine if Twist was also mediating the acquisition of metastatic powers following E-cadherin down-regulation, we evaluated the metastatic ability of Twist-inhibited cells using the experimental metastasis assay. Whereas control shEcad cells were able to efficiently colonize the lung, as before, cells doubly inhibited for E-cadherin and Twist exhibited a marked decrease in the ability to do so (Fig. 6D). Collectively, these results indicate that Twist is a crucial downstream effector of cellular functions in response to E-cadherin loss and is necessary for the metastasis of E-cadherin–deficient cells.

Discussion

In this study, we show that the loss of E-cadherin has wide-ranging transcriptional and functional consequences for human breast epithelial cells. In fact, E-cadherin loss is sufficient to confer metastatic ability on breast cancer cells that are otherwise essentially nonmetastatic. Moreover, by using a dominant-negative E-cadherin mutant, we show that the acquisition of metastatic ability by cancer cells following E-cadherin loss is not attributable solely to the disruption of intercellular adhesion contacts. Instead, it is the additional loss of E-cadherin protein that provokes an EMT, attended by increased cellular motility, invasiveness, and resistance to apoptosis.

The mechanisms by which E-cadherin is inactivated in human tumors can be placed into two general categories: (*a*) those that
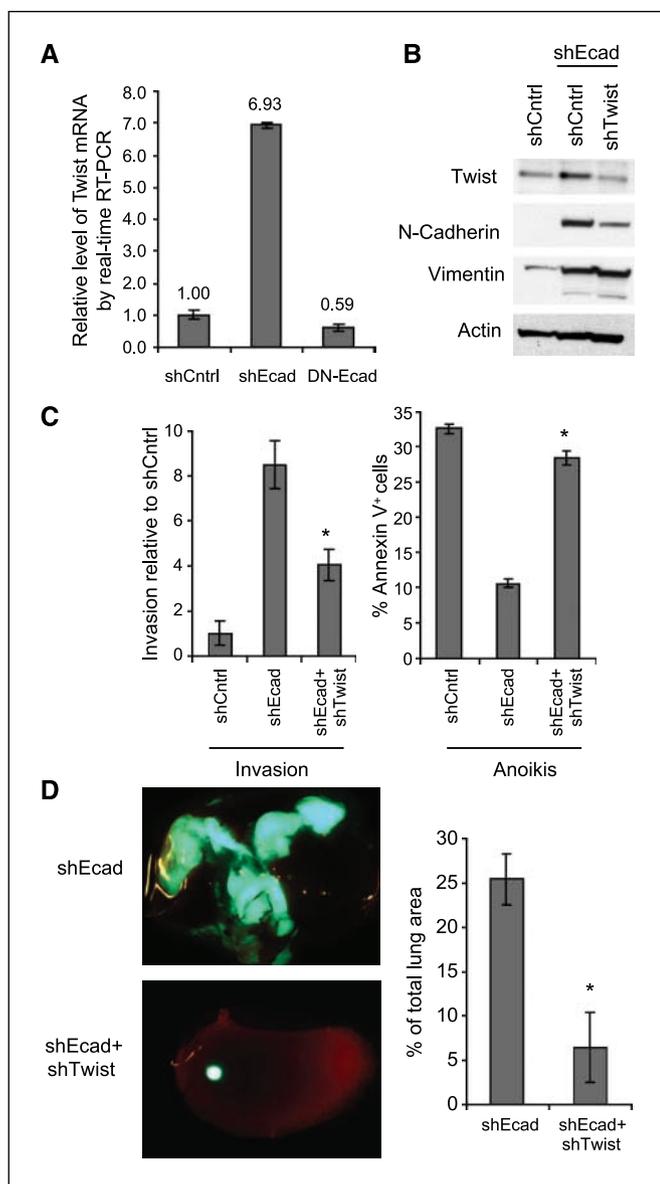
---

[10] Manuscript in preparation.

Figure 6. Twist is up-regulated on loss of E-cadherin and plays a functionally important role in E-cadherin loss–induced EMT and metastasis. *A,* the relative levels of *twist* mRNA measured by real-time RT-PCR in HMLER-shEcad and DN-Ecad cells compared with shCntrl cells. *Columns,* mean from triplicate PCRs; *bars,* SE. *B,* expression levels of twist, vimentin, and N-cadherin in HMLER-shCntrl, shEcad, and double knockdown cells (shEcad + shTwist). β-Actin is used as a loading control. *C, right,* HMLER-shCntrl, shEcad, and shEcad + shTwist cells were induced to invade through Matrigel-coated transwell membranes. After 16 h, the invaded cells were fixed, stained, photographed, and counted. *Columns,* mean of triplicate assays, shown relative to shCntrl cell invasion; *bars,* SD. *, $P < 0.01$, compared with shEcad. *Left,* the percentage of apoptotic HMLER-shCntrl, shEcad, and shEcad + shTwist cells in suspension were determined by binding of FITC-conjugated Annexin V. The FACS analyses were done 24 h after suspension culture. *Columns,* mean number of Annexin V–positive cells expressed as a percentage of total cells; *bars,* SD. *, $P < 0.01$, compared with shEcad. *D,* representative fluorescence images of mouse lung lobes 8 wk after tail-vein injection of shEcad or shEcad + shTwist cells. GFP signal denotes the presence of tumor cells (*left*). *Right,* quantification of total lung metastasis burden in the same sets of mice. *Columns,* mean of five mice analyzed; *bars,* SD. *, $P < 0.01$.

result in the production of a nonfunctional protein and (*b*) those that lead to the complete absence of E-cadherin. The present results suggest that point mutations in the extracellular domain that preserve the cytoplasmic tail of E-cadherin (18) are not likely

to result in an EMT or to afford functional traits that allow completion of the later steps of metastasis. In contrast, complete elimination of E-cadherin expression (occurring in human tumors via truncation mutation or locus repression/loss*)* results in the activation of the malignancy-associated traits listed above. Stated differently, loss of E-cadherin, in combination with certain additional oncogenic lesions, results in the acquisition of multiple functional traits that contribute to the completion of several rate-limiting steps in the invasion-metastasis cascade.

A recent study has shown that combined loss of p53 and E-cadherin in the mouse mammary gland results in metastatic tumors that, in contrast to our findings, do not exhibit a "classic" EMT phenotype (5). However, in concordance with our results, cells from such tumors were highly resistant to anoikis. This suggests that differences between the mouse and human mammary glands, the cell types targeted, and the (epi)genetic constitutions of such cells may play an important role in determining the phenotypic response to E-cadherin loss.

In our human mammary epithelial cell system, the retention of the cytoplasmic tail of E-cadherin prevented EMT induction; therefore, we initially focused our efforts on proteins known to bind this cytoplasmic domain, specifically β-catenin. In addition to the release of β-catenin from cell adherens junctions, loss of E-cadherin led to inactivation of GSK3β through phosphorylation. In the future, it will be interesting to explore the signaling pathways that are induced by loss of E-cadherin to inactivate GSK3β, thus further stabilizing the released β-catenin.

Although we found β-catenin to be necessary for several aspects of E-cadherin loss–induced EMT, it was not sufficient to cause these phenotypes. Therefore, we concluded that additional signals beyond those conveyed by β-catenin must be important in transducing the downstream effects of E-cadherin loss. Others have reported that the adherens junction–associated proteins α-catenin and p120 catenin may also modulate intracellular signaling pathways (11, 12); however, we have been unable to find evidence for the activation of signaling pathways by either of these two proteins following E-cadherin loss (data not shown).

We therefore undertook to identify the spectrum of transcriptional changes resulting from E-cadherin loss. Expression profiling revealed that 19 transcription factors were highly induced following E-cadherin loss, all of which did not ostensibly require β-catenin for their induction. Interestingly, Twist and ZEB-1, both previously known to cause E-cadherin repression, were among the transcription factors up-regulated following E-cadherin loss (22, 44). This means that in some cells, transient E-cadherin loss may result in the induction of its own repressors, yielding a feed-forward signaling loop whereby the EMT-induced mesenchymal state, once established, is stabilized and perhaps maintained. Thus, E-cadherin can act as a central modulator of the cell biological phenotypes and the molecular factors that govern metastatic dissemination of carcinomas.

Disclosure of Potential Conflicts of Interest

No potential conflicts of interest were disclosed.

Acknowledgments

References

1. Gupta GP, Massague J. Cancer metastasis: building a framework. Cell 2006;127:679–95.

2. Oka H, Shiozaki H, Kobayashi K, et al. Expression of E-cadherin cell adhesion molecules in human breast cancer tissues and its relationship to metastasis. Cancer Res 1993;53:1696–701.

3. Schipper JH, Frixen UH, Behrens J, Unger A, Jahnke K, Birchmeier W. E-Cadherin expression in squamous cell carcinomas of head and neck: inverse correlation with tumor dedifferentiation and lymph node metastasis. Cancer Res 1991;51:6328–37.

4. Umbas R, Isaacs WB, Bringuier PP, et al. Decreased E-cadherin expression is associated with poor prognosis in patients with prostate cancer. Cancer Res 1994;54:3929–33.

5. Derksen PW, Liu X, Saridin F, et al. Somatic inactivation of E-cadherin and p53 in mice leads to metastatic lobular mammary carcinoma through induction of anoikis resistance and angiogenesis. Cancer Cell 2006;10:437–49.

6. Perl AK, Wilgenbus P, Dahl U, Semb H, Christofori G. A causal role for E-cadherin in the transition from adenoma to carcinoma. Nature 1998;392:190–3.

7. Frixen UH, Behrens J, Sachs M, et al. E-Cadherin-mediated cell-cell adhesion prevents invasiveness of human carcinoma cells. J Cell Biol 1991;113:173–85.

8. Vleminckx K, Vakaet L, Jr., Mareel M, Fiers W, van Roy F. Genetic manipulation of E-cadherin expression by epithelial tumor cells reveals an invasion suppressor role. Cell 1991;66:107–19.

9. Nagafuchi A, Shirayoshi Y, Okazaki K, Yasuda K, Takeichi M. Transformation of cell adhesion properties by exogenously introduced E-cadherin cDNA. Nature 1987;329:341–3.

10. Gumbiner BM. Regulation of cadherin-mediated adhesion in morphogenesis. Nat Rev Mol Cell Biol 2005;6:622–34.

11. Wildenberg GA, Dohn MR, Carnahan RH, et al. p120-catenin and p190RhoGAP regulate cell-cell adhesion by coordinating antagonism between Rac and Rho. Cell 2006;127:1027–39.

12. Vasioukhin V, Bauer C, Degenstein L, Wise B, Fuchs E. Hyperproliferation and defects in epithelial polarity on conditional ablation of α-catenin in skin. Cell 2001; 104:605–17.

13. Nelson WJ, Nusse R. Convergence of Wnt, β-catenin, and cadherin pathways. Science 2004;303:1483–7.

14. Perez-Moreno M, Fuchs E. Catenins: keeping cells from getting their signals crossed. Dev Cell 2006;11: 601–12.

15. Hirohashi S. Inactivation of the E-cadherin-mediated cell adhesion system in human cancers. Am J Pathol 1998;153:333–9.

16. Strathdee G. Epigenetic versus genetic alterations in the inactivation of E-cadherin. Semin Cancer Biol 2002; 12:373–9.

17. Maretzky T, Reiss K, Ludwig A, et al. ADAM10 mediates E-cadherin shedding and regulates epithelial cell-cell adhesion, migration, and β-catenin translocation. Proc Natl Acad Sci U S A 2005;102:9182–7.

18. Berx G, Becker KF, Hofler H, van Roy F. Mutations of the human E-cadherin (CDH1) gene. Hum Mutat 1998; 12:226–37.

19. Yoshiura K, Kanai Y, Ochiai A, Shimoyama Y, Sugimura T, Hirohashi S. Silencing of the E-cadherin invasion-suppressor gene by CpG methylation in human carcinomas. Proc Natl Acad Sci U S A 1995; 92:7416–9.

20. Bolos V, Peinado H, Perez-Moreno MA, Fraga MF, Esteller M, Cano A. The transcription factor Slug represses E-cadherin expression and induces epithelial to mesenchymal transitions: a comparison with Snail and E47 repressors. J Cell Sci 2003;116:499–511.

21. Batlle E, Sancho E, Franci C, et al. The transcription factor snail is a repressor of E-cadherin gene expression in epithelial tumour cells. Nat Cell Biol 2000;2:84–9.

22. Yang J, Mani SA, Donaher JL, et al. Twist, a master regulator of morphogenesis, plays an essential role in tumor metastasis. Cell 2004;117:927–39.

23. Thiery JP, Sleeman JP. Complex networks orchestrate epithelial-mesenchymal transitions. Nat Rev Mol Cell Biol 2006;7:131–42.

24. Huber MA, Kraut N, Beug H. Molecular requirements for epithelial-mesenchymal transition during tumor progression. Curr Opin Cell Biol 2005;17:548–58.

25. Elenbaas B, Spirio L, Koerner F, et al. Human breast cancer cells generated by oncogenic transformation of primary mammary epithelial cells. Genes Dev 2001;15: 50–65.

26. Stewart SA, Dykxhoorn DM, Palliser D, et al. Lentivirus-delivered stable gene silencing by RNAi in primary cells. RNA 2003;9:493–501.

27. Hartwell KA, Muir B, Reinhardt F, Carpenter AE, Sgroi DC, Weinberg RA. The Spemann organizer gene, Goosecoid, promotes tumor metastasis. Proc Natl Acad Sci U S A 2006;103:18969–74.

28. Rasband WS. ImageJ. Bethesda (MD): U.S. National Institutes of Health; 1997–2006.

29. Team RDC. R: a language and environment for statistical computing. Vienna (Austria): R Foundation for Statistical Computing; 2007.

30. Dahl U, Sjodin A, Semb H. Cadherins regulate aggregation of pancreatic β-cells *in vivo*. Development 1996;122:2895–902.

31. Martin SS, Ridgeway AG, Pinkas J, et al. A cytoskeleton-based functional genetic screen identifies Bcl-xL as an enhancer of metastasis, but not primary tumor growth. Oncogene 2004;23:4641–5.

32. Douma S, Van Laar T, Zevenhoven J, Meuwissen R, Van Garderen E, Peeper DS. Suppression of anoikis and induction of metastasis by the neurotrophic receptor TrkB. Nature 2004;430:1034–9.

33. Kim K, Lu Z, Hay ED. Direct evidence for a role of β-catenin/LEF-1 signaling pathway in induction of EMT. Cell Biol Int 2002;26:463–76.

34. Yang L, Lin C, Liu ZR. P68 RNA helicase mediates PDGF-induced epithelial mesenchymal transition by displacing Axin from β-catenin. Cell 2006;127:139–55.

35. Eger A, Stockinger A, Park J, et al. β-Catenin and TGFβ signalling cooperate to maintain a mesenchymal phenotype after FosER-induced epithelial to mesenchymal transition. Oncogene 2004;23:2672–80.

36. Morali OG, Delmas V, Moore R, Jeanney C, Thiery JP, Larue L. IGF-II induces rapid β-catenin relocation to the nucleus during epithelium to mesenchyme transition. Oncogene 2001;20:4942–50.

37. Liebner S, Cattelino A, Gallini R, et al. β-Catenin is required for endothelial-mesenchymal transformation during heart cushion development in the mouse. J Cell Biol 2004;166:359–67.

38. Conacci-Sorrell M, Simcha I, Ben-Yedidia T, Blechman J, Savagner P, Ben-Ze'ev A. Autoregulation of E-cadherin expression by cadherin-cadherin interactions: the roles of β-catenin signaling, Slug, and MAPK. J Cell Biol 2003; 163:847–57.

39. Cross DA, Alessi DR, Cohen P, Andjelkovich M, Hemmings BA. Inhibition of glycogen synthase kinase-3 by insulin mediated by protein kinase B. Nature 1995; 378:785–9.

40. Dennis G, Jr., Sherman BT, Hosack DA, et al. DAVID: database for annotation, visualization, and integrated discovery. Genome Biol 2003;4:P3.

41. Grooteclaes ML, Frisch SM. Evidence for a function of CtBP in epithelial gene regulation and anoikis. Oncogene 2000;19:3823–8.

42. Cano A, Perez-Moreno MA, Rodrigo I, et al. The transcription factor snail controls epithelial-mesenchymal transitions by repressing E-cadherin expression. Nat Cell Biol 2000;2:76–83.

43. Comijn J, Berx G, Vermassen P, et al. The two-handed E box binding zinc finger protein SIP1 down-regulates E-cadherin and induces invasion. Mol Cell 2001;7:1267–78.

44. Eger A, Aigner K, Sonderegger S, et al. ΔEF1 is a transcriptional repressor of E-cadherin and regulates epithelial plasticity in breast cancer cells. Oncogene 2005;24:2375–85.

Loss of E-Cadherin Promotes Metastasis via Multiple Downstream Transcriptional Pathways

Tamer T. Onder, Piyush B. Gupta, Sendurai A. Mani, et al.

Updated version	Access the most recent version of this article at: http://cancerres.aacrjournals.org/content/68/10/3645
Supplementary Material	Access the most recent supplemental material at: http://cancerres.aacrjournals.org/content/suppl/2008/05/12/68.10.3645.DC1

Cited articles	This article cites 42 articles, 14 of which you can access for free at: http://cancerres.aacrjournals.org/content/68/10/3645.full#ref-list-1
Citing articles	This article has been cited by 100 HighWire-hosted articles. Access the articles at: http://cancerres.aacrjournals.org/content/68/10/3645.full#related-urls

E-mail alerts	Sign up to receive free email-alerts related to this article or journal.
Reprints and Subscriptions	To order reprints of this article or to subscribe to the journal, contact the AACR Publications Department at pubs@aacr.org.
Permissions	To request permission to re-use all or part of this article, use this link http://cancerres.aacrjournals.org/content/68/10/3645. Click on "Request Permissions" which will take you to the Copyright Clearance Center's (CCC) Rightslink site.